Preprints of the 21st IFAC World Congress (Virtual)
Berlin, Germany, July 12-17, 2020

Adaptive tracking control for quadrotors without linear velocity measurements ⋆

Jonathan Hirata-Acosta * **Javier Pliego-Jiménez** *,** **César Cruz-Hernández** *

* *Departamento de Electrónica y Telecomunicaciones, División de Física Aplicada, CICESE, Ensenada, B.C. México,22860 (email: jhirata@cicese.edu.mx, ccruz@cicese.mx)*
** *Consejo Nacional de Ciencia y Tecnología, Cd. Mx. México, 03940 (e-mail: jpliego@cicese.mx)*

Abstract: The problem of trajectory tracking of a quadrotor without using linear velocity measurements and with model parameter uncertainties is addressed in this paper. A linear observer is proposed to overcome the problem of a lack of linear velocity measurements. The proposed adaptive control algorithm exploits the cascade structure of the translational and attitude dynamics of the quadrotor and guarantees asymptotic convergence of the tracking and observer errors. The attitude control is designed based on the unit quaternion; thus, the well-known singularities of the Euler angles are avoided. Simulation results are presented to show the performance of the proposed control scheme.

Keywords: Quadrotor, Luenberger Observer, Adaptive Control, Cascade Systems, Unit Quaternion.

1. INTRODUCTION

A quadrotor is an aircraft composed of four rotors that can perform vertical take-off, landing, and hovering flight maneuvers. Such capabilities allow this type of aerial robot to carry out several tasks, for instance, surveillance, exploration, 3D-mapping, transportation, for mention a few. Therefore, the interest in modeling and controlling quadrotors has rapidly grown in recent years (Castillo et al., 2005; Mahoney et al., 2012).

Quadrotors are under-actuated nonlinear systems with six degrees of freedom; therefore, the trajectory tracking and pose regulation problems for these systems are challenging tasks. Nevertheless, in a variety of applications, the aircraft operates near the hovering regime, in this case, the quadrotor's dynamic can be approximated by a linear system (Michael et al., 2010), and several linear control algorithms have been proposed (Bouabdallah et al., 2004; Pounds et al., 2006).

To overcome the limitations of linear controllers, nonlinear control algorithms and trajectory planning methods that allows the quadrotor to perform complex and aggressive maneuvers have been proposed in the literature (Lee et al., 2009; Zuo, 2010; Mellinger et al., 2012). The attitude stabilization problem was addressed in (Tayebi and McGilvray, 2006) where a unit quaternion-based feedback controller with exponential convergence property was proposed. Kendoul et al. (2010) proposed a hierarchical model-based nonlinear control that achieves stabilization and trajectory tracking. The control algorithm relies on the extraction of the desired Euler angles and total thrust from a intermediary control input. On the other hand, Lee et al. (2010) proposed a novel almost global nonlinear geometric control on $SE(3)$. Simulation results show that this controller can be use to perform aggressive maneuvers. Nevertheless, the aforementioned control schemes assume full-state measurements. Moreover, it is assumed that the quadrotor's dynamic parameters are known.

Due to hardware limitations, it is not always possible to measure all the state variables of the aircraft. To circumvent the problem of lack of state measurements several researches have been proposed velocity observers, linear and nonlinear filters. Rosaldo-Serrano et al. (2019) proposed a Luenberger observer to estimate both the linear and angular velocity of the system. The observer was used in combination with a backstepping control algorithm for trajectory tracking of a group of AR.drone quadrotors. A nonlinear velocity observer and a nonlinear controller based on the unit quaternion is proposed in (Abdessameud and Tayebi, 2010). The observer only estimates the linear velocity and the complete control-observer scheme achieves global trajectory tracking. A nonlinear controller without linear and angular velocity measuremntes based on nonlinear filters is proposed in (Zou, 2017b).

On the other hand, the problem of model parameters uncertainties is addressed in (Ha et al., 2014) and (Zou, 2017a). In the former work it is assumed that the mass of aircraft is unknown and a passivity-based adaptive backstepping control is proposed. In the latter, a robust nonlinear adaptive control is presented which deals with a mass and inertia matrix uncertainties. A model reference adaptive control (MARC) for trajectory tracking for a

⋆ This work was funded by the internal project F0F156 "Generation of collective behaviors and their applications" and the CONACyT Basic Science project A1-S-31628. We extend our thanks to CONACyT for the financial support that allows us to do our research work.

low-cost quadrotor is proposed in (Dydek et al., 2013). The controller's performance was successfully validate by means of experimental test on the RAVEN laboratory platform (How et al., 2008).

In this paper a nonlinear adaptive control algorithm is proposed for trajectory tracking of quadrotor in a 3D environment without using linear velocity measurements. The controller exploits the cascade structure of the equations of motion of the aircraft. As a result, a hierarchical control strategy is adopted. First, an auxiliary control is proposed to achieve trajectory position tracking. Such auxiliary control allows us to compute the total thrust and the desired orientation (outer-loop control). Once the desired attitude is obtained, a nonlinear adaptive control is designed for the quadrotor's attitude dynamics (inner-loop control). The linear velocity is estimated by means of a simple Luenberger observer. The remaining sections of the paper are organized as follows: Section 2 presents the dynamic model and kinematic relationships of the quadrotor. The linear velocity observer is introduced in Section 3. The proposed control scheme as well as the stability analysis of the closed-loop system is presented in Section 4. Simulations results are given in Section 5. Finally, some concluding remarks are discussed in Section 6.

2. DYNAMIC MODEL

In this section, the equations of motion of the quadrotor are presented. Let $\Sigma_0 = \{\boldsymbol{x}_0, \boldsymbol{y}_0, \boldsymbol{z}_0\}$ be the inertial frame and let $\Sigma_1 = \{\boldsymbol{x}_1, \boldsymbol{y}_1, \boldsymbol{z}_1\}$ be a second frame attached to the center of mass of the quadrotor. The frames Σ_0 and Σ_1 are related by the rotation matrix $\boldsymbol{R} \in SO(3)$ which describes the orientation of the quadrotor. According to Fig. 1, $\boldsymbol{p} \in \Re^3$ and $\boldsymbol{v} = \dot{\boldsymbol{p}} \in \Re^3$ denote, respectively, the position and linear velocity of the quadrotor's center of mass expressed w.r.t. the inertial frame Σ_0, and $\boldsymbol{\omega} \in \Re^3$ denotes the angular velocity expressed w.r.t. the body frame Σ_1. The equations of motion of the system are given by

$$\begin{aligned} \dot{\boldsymbol{p}} &= \boldsymbol{v} \\ \dot{\boldsymbol{v}} &= \frac{\mathcal{T}}{m}\boldsymbol{R}\boldsymbol{z}_0 - g\boldsymbol{z}_0 \end{aligned} \quad (1)$$

$$\begin{aligned} \dot{\boldsymbol{R}} &= \boldsymbol{R}\boldsymbol{S}(\boldsymbol{\omega}) \\ \boldsymbol{J}\dot{\boldsymbol{\omega}} &= \boldsymbol{\tau} - \boldsymbol{S}(\boldsymbol{\omega})\boldsymbol{J}\boldsymbol{\omega} \end{aligned} \quad (2)$$

where g, m and $\boldsymbol{J} \in \Re^{3\times3}$ are, respectively, the gravity constant, the mass and constant inertia matrix of the quadcopter, $\mathcal{T} \in \Re$ and $\boldsymbol{\tau} \in \Re^3$ denote the total thrust and the external input torque. Finally, $\boldsymbol{S}(\cdot) \in \Re^{3\times3}$ is a skew-symmetric matrix which satisfies $\boldsymbol{S}(\boldsymbol{q}_1)\boldsymbol{q}_2 = \boldsymbol{q}_1 \times \boldsymbol{q}_2$ and $\|\boldsymbol{S}(\boldsymbol{q}_1)\| = \|\boldsymbol{q}_1\|\ \forall\, \boldsymbol{q}_1, \boldsymbol{q}_2 \in \Re^3$ where $\times$ denotes the cross product operator.

Alternatively to the rotation matrix $\boldsymbol{R}$, the attitude of the quadrotor can be described by the four-parameter unit quaternion denoted by $\mathcal{Q} = \{\eta, \boldsymbol{\epsilon}\}$, where $\eta \in \Re$ and $\boldsymbol{\epsilon} = \mathrm{col}(\epsilon_{\mathrm{x}}, \epsilon_{\mathrm{y}}, \epsilon_{\mathrm{z}}) \in \Re^3$ denote the scalar and vector parts, respectively. The unit quaternion presents the following properties: $\eta^2 + \boldsymbol{\epsilon}^{\mathrm{T}}\boldsymbol{\epsilon} = 1$ and $\mathcal{Q}^{-1} = \{1, -\boldsymbol{\epsilon}\}$ where $\mathcal{Q}^{-1}$ denotes the inverse of $\mathcal{Q}$. Given the unit quaternions $\mathcal{Q}_1 = \{\eta_1, \boldsymbol{\epsilon}_1\}$ and $\mathcal{Q}_2 = \{\eta_2, \boldsymbol{\epsilon}_2\}$, the quaternion product is defined as $\mathcal{Q}_1 \otimes \mathcal{Q}_2 = \left\{\eta_1\eta_2 - \boldsymbol{\epsilon}_1^{\mathrm{T}}\boldsymbol{\epsilon}_2, \eta_1\boldsymbol{\epsilon}_2 + \eta_2\boldsymbol{\epsilon}_1 + \boldsymbol{S}(\boldsymbol{\epsilon}_1)\boldsymbol{\epsilon}_2\right\}$ is equivalent to the rotation matrix multiplication $\boldsymbol{R}_1\boldsymbol{R}_2$.

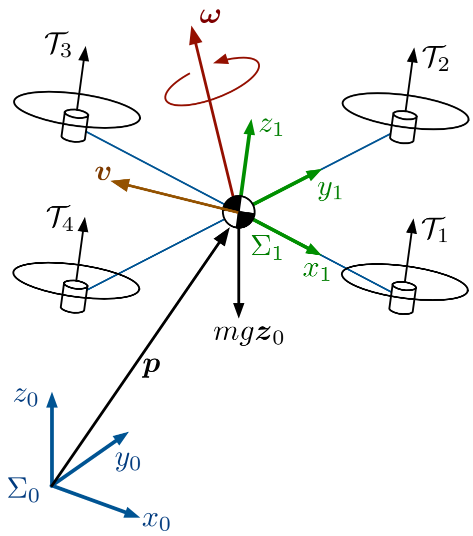

Fig. 1. Quadrotor composed of four rotors, $\mathcal{T} = \sum_{i=1}^{4} \mathcal{T}_i$ and $\boldsymbol{\tau}$ are the control inputs

The rotation matrix corresponding to a given quaternion is $\boldsymbol{R}(\eta, \boldsymbol{\epsilon}) = (2\eta^2 - 1)\boldsymbol{I} + 2\boldsymbol{\epsilon}\boldsymbol{\epsilon}^{\mathrm{T}} + 2\eta\boldsymbol{S}(\boldsymbol{\epsilon})$, therefore, $\boldsymbol{R}^{\mathrm{T}}\boldsymbol{R} = \boldsymbol{I} \Leftrightarrow \mathcal{Q}^{-1}\mathcal{Q} = \{1, \boldsymbol{0}\}$. Finally, the time-derivative of $\mathcal{Q} = \{\eta, \boldsymbol{\epsilon}\}$ is related to the angular velocity $\boldsymbol{\omega}$ by the so-called propagation rule (Siciliano and Villani, 1999)

$$\begin{aligned} \dot{\eta} &= -\frac{1}{2}\boldsymbol{\epsilon}^{\mathrm{T}}\boldsymbol{\omega} \\ \dot{\boldsymbol{\epsilon}} &= \frac{1}{2}\left(\eta\boldsymbol{I} - \boldsymbol{S}(\boldsymbol{\epsilon})\right)\boldsymbol{\omega}. \end{aligned} \quad (3)$$

3. LINEAR VELOCITY OBSERVER

Commercial quadrotors are equipped with inertial measurement units (IMUs) composed of gyroscopes, accelerometers, and magnetometers. Such devices allows to measure the angular velocity and attitude of the quadrotor. The position can be measured by means of infrared, acoustic, barometric sensors, global positioning system (GPS) or VICON systems. Nevertheless, the problem of measuring the linear velocity is more cumbersome. This drawback motive us to propose an algorithm to estimate the linear velocity of the aerial vehicle. Assuming that $\boldsymbol{p}$ and $\boldsymbol{R}$ are available from measurements, the proposed velocity observer for the subsystem (1) is given by

$$\begin{aligned} \dot{\widehat{\boldsymbol{p}}} &= \widehat{\boldsymbol{v}} + \boldsymbol{L}_1\widetilde{\boldsymbol{p}} \\ \dot{\widehat{\boldsymbol{v}}} &= \frac{\mathcal{T}}{m}\boldsymbol{R}\boldsymbol{z}_0 - g\boldsymbol{z}_0 + \boldsymbol{L}_2\widetilde{\boldsymbol{p}} \end{aligned} \quad (4)$$

where $\widetilde{\boldsymbol{p}} \triangleq \boldsymbol{p} - \hat{\boldsymbol{p}}$ is the observation error, $\widehat{\boldsymbol{p}}$ denotes the estimate of $\boldsymbol{p}$ and $\boldsymbol{L}_1$, $\boldsymbol{L}_2 \in \Re^{3\times3}$ are positive definite matrices. By taking into account (1) and (4) the time-derivative of the observation errors $\widetilde{\boldsymbol{p}}$ and $\widetilde{\boldsymbol{v}} = \boldsymbol{v} - \widehat{\boldsymbol{v}}$ are given by

$$\begin{aligned} \dot{\widetilde{\boldsymbol{p}}} &= -\boldsymbol{L}_1\widetilde{\boldsymbol{p}} + \widetilde{\boldsymbol{v}} \\ \dot{\widetilde{\boldsymbol{v}}} &= -\boldsymbol{L}_2\widetilde{\boldsymbol{p}}, \end{aligned} \quad (5)$$

which is equivalent to

$$\ddot{\widetilde{\boldsymbol{p}}} + \boldsymbol{L}_1\dot{\widetilde{\boldsymbol{p}}} + \boldsymbol{L}_2\widetilde{\boldsymbol{p}} = \boldsymbol{0}. \quad (6)$$

Since the observer gains $\boldsymbol{L}_1$ and $\boldsymbol{L}_2$ are positive definite matrices, the equilibrium point $(\widetilde{\boldsymbol{p}}, \widetilde{\boldsymbol{v}}) = (\boldsymbol{0}, \boldsymbol{0})$ is asymptotically (exponentially) stable.

4. CONTROL ALGORITHM DESIGN

The dynamic model of the quadrotor presents a cascade structure where the interconnection term $m^{-1}\mathcal{T}\boldsymbol{R}\boldsymbol{z}_0$ relates the rotational dynamics (2) with the translational equation of motion (1). Moreover, eq. (2) is independent of the states $\boldsymbol{p}$ and $\boldsymbol{v}$. Such characteristic allows us to apply a hierarchical control strategy. The basic idea is to use the total thrust and the quadrotor's attitude as the control inputs for the position subsystem.

4.1 Position controller

Consider the auxiliary control input

$$\boldsymbol{u} = \frac{\mathcal{T}}{m}\boldsymbol{R}_{\mathrm{d}}\boldsymbol{z}_0 - g\boldsymbol{z}_0 = \frac{\mathcal{T}}{m}\begin{bmatrix} 2(\epsilon_{\mathrm{xd}}\epsilon_{\mathrm{zd}} + \eta_{\mathrm{d}}\epsilon_{\mathrm{yd}}) \\ 2(\epsilon_{\mathrm{yd}}\epsilon_{\mathrm{zd}} - \eta_{\mathrm{d}}\epsilon_{\mathrm{xd}}) \\ 2(\eta_{\mathrm{d}}^2 + \epsilon_{\mathrm{zd}}^2) - 1 \end{bmatrix} - g\boldsymbol{z}_0 \quad (7)$$

where $\boldsymbol{R}_{\mathrm{d}} = \boldsymbol{R}_{\mathrm{d}}(\eta_{\mathrm{d}}, \boldsymbol{\epsilon}_{\mathrm{d}})$ is the desired rotation matrix. Therefore, given $\boldsymbol{u} = \mathrm{col}(u_{\mathrm{x}}, u_{\mathrm{y}}, u_{\mathrm{z}})$ it is possible to compute the total thrust $\mathcal{T}$ and the desired attitude $\mathcal{Q}_{\mathrm{d}} = \{\eta_{\mathrm{d}}, \boldsymbol{\epsilon}_{\mathrm{d}}\}$. By exploiting the properties of rotation matrices, one has

$$\mathcal{T} = m\left\|\boldsymbol{u} + g\boldsymbol{z}_0\right\|_2. \quad (8)$$

In order to compute η_{d} and $\boldsymbol{\epsilon}_{\mathrm{d}}$, the value of ϵ_{zd} is fixed to zero, hence

$$\eta_{\mathrm{d}} = \left[\frac{1}{2} + \frac{m(u_{\mathrm{z}} + g)}{2\mathcal{T}}\right]^{\frac{1}{2}}, \quad \boldsymbol{\epsilon}_{\mathrm{d}} = \frac{m}{2\eta_{\mathrm{d}}\mathcal{T}}\begin{bmatrix} -u_{\mathrm{y}} \\ u_{\mathrm{x}} \\ 0 \end{bmatrix} \quad (9)$$

under the condition that $\boldsymbol{u} \neq \mathrm{col}(0, 0, -g)$ (see (Abdessameud and Tayebi, 2009) for further details). The auxiliary control input $\boldsymbol{u}$ is proposed as follows

$$\begin{aligned}\boldsymbol{u} &= \dot{\boldsymbol{v}}_{\mathrm{d}} + \boldsymbol{K}_1(\boldsymbol{p}_{\mathrm{d}} - \widehat{\boldsymbol{p}}) + \boldsymbol{K}_2(\boldsymbol{v}_{\mathrm{d}} - \widehat{\boldsymbol{v}}) \\ &= \dot{\boldsymbol{v}}_{\mathrm{d}} + \boldsymbol{K}_1\Delta\boldsymbol{p} + \boldsymbol{K}_2\Delta\boldsymbol{v} + \boldsymbol{K}_1\widetilde{\boldsymbol{p}} + \boldsymbol{K}_2\widetilde{\boldsymbol{v}}\end{aligned} \quad (10)$$

where $\boldsymbol{K}_1$, $\boldsymbol{K}_2 \in \Re^{3\times 3}$ are positive definite matrices, $\boldsymbol{p}_{\mathrm{d}} \in \Re^3$ is the desired position with $\boldsymbol{v}_{\mathrm{d}} = \dot{\boldsymbol{p}}_{\mathrm{d}}$, $\dot{\boldsymbol{v}}_{\mathrm{d}} = \ddot{\boldsymbol{p}}_{\mathrm{d}}$ and $\Delta\boldsymbol{p} \triangleq \boldsymbol{p}_{\mathrm{d}} - \boldsymbol{p}$, $\Delta\boldsymbol{v} \triangleq \boldsymbol{v}_{\mathrm{d}} - \boldsymbol{v}$ are the position and velocity tracking errors. Based on (9) and (10), the desired angular velocity can be computed as

$$\boldsymbol{\omega}_{\mathrm{d}} = 2\begin{bmatrix} -\boldsymbol{\epsilon}_{\mathrm{d}}^{\mathrm{T}} \\ \eta_{\mathrm{d}}\boldsymbol{I} - \boldsymbol{S}(\boldsymbol{\epsilon}_{\mathrm{d}}) \end{bmatrix}^{\mathrm{T}} \begin{bmatrix} \dot{\eta}_{\mathrm{d}} \\ \dot{\boldsymbol{\epsilon}}_{\mathrm{d}} \end{bmatrix} \quad (11)$$

where $\dot{\eta}_{\mathrm{d}}$, $\dot{\boldsymbol{\epsilon}}_{\mathrm{d}}$ are obtained by differentiating (9). To avoid complex calculations, the time-derivative of $\boldsymbol{\omega}_{\mathrm{d}}$ can be approximated by a low-pass filter $\dot{\boldsymbol{\omega}}_{\mathrm{d}} = \frac{s}{\lambda s + 1}\boldsymbol{\omega}_{\mathrm{d}}$ with $\lambda > 0$ is the cutoff frequency.

4.2 Attitude controller

The next step of the hierarchical control strategy is to design the control torque input $\boldsymbol{\tau}$ that guarantees the trajectory tracking of the desired attitude $\mathcal{Q}_{\mathrm{d}} = \{\eta_{\mathrm{d}}, \boldsymbol{\epsilon}_{\mathrm{d}}\}$. To this end, the following property of the attitude dynamics (2) will be exploited:

Property 1. The attitude dynamics described by (2) is linear w.r.t. the inertial parameters, *i.e.*,

$$\boldsymbol{J}\dot{\boldsymbol{\omega}} + \boldsymbol{S}(\boldsymbol{\omega})\boldsymbol{J}\boldsymbol{\omega} = \boldsymbol{Y}(\boldsymbol{\omega}, \dot{\boldsymbol{\omega}})\boldsymbol{\theta} = \boldsymbol{\tau} \quad (12)$$

where $\boldsymbol{\theta} \in \Re^p$ is the inertial parameter vector and $\boldsymbol{Y}(\boldsymbol{\omega}, \dot{\boldsymbol{\omega}}) \in \Re^{3\times p}$ is called the regressor matrix. □

The attitude error is defined as

$$\Delta\mathcal{Q} = \{\Delta\eta, \Delta\boldsymbol{\epsilon}\} = \mathcal{Q}^{-1} \otimes \mathcal{Q}_{\mathrm{d}}. \quad (13)$$

Therefore, the quadrotor's attitude $\boldsymbol{R}$ is aligned to the desired attitude $\boldsymbol{R}_{\mathrm{d}}$ when $\Delta\mathcal{Q} = \{1, \boldsymbol{0}\}$. In terms of rotation matrix, the attitude error is given by $\Delta\boldsymbol{R}(\Delta\eta, \Delta\boldsymbol{\epsilon}) = \boldsymbol{R}^{\mathrm{T}}\boldsymbol{R}_{\mathrm{d}}$. The angular velocity error is given by

$$\Delta\boldsymbol{\omega} = \bar{\boldsymbol{\omega}}_{\mathrm{d}} - \boldsymbol{\omega}. \quad (14)$$

where $\bar{\boldsymbol{\omega}}_{\mathrm{d}} \triangleq \Delta\boldsymbol{R}(\Delta\eta, \Delta\boldsymbol{\epsilon})\boldsymbol{\omega}_{\mathrm{d}}$. Before presenting the attitude controller, consider the following auxiliary variables

$$\boldsymbol{\omega}_{\mathrm{r}} = \bar{\boldsymbol{\omega}}_{\mathrm{d}} + k_\epsilon\Delta\boldsymbol{\epsilon} \quad (15)$$

$$\boldsymbol{\xi} = \boldsymbol{\omega}_{\mathrm{r}} - \boldsymbol{\omega} = \Delta\boldsymbol{\omega} + k_\epsilon\Delta\boldsymbol{\epsilon} \quad (16)$$

where $\boldsymbol{\omega}_{\mathrm{r}} \in \Re^3$ is a reference velocity signal and $\boldsymbol{\xi} \in \Re^3$ is an error variable.

Based on the previous definition and by taking into account (3), (12)-(16) the attitude dynamics can be written as

$$\begin{aligned}\Delta\dot{\eta} &= -\frac{1}{2}\Delta\boldsymbol{\epsilon}^{\mathrm{T}}\Delta\boldsymbol{\omega} \\ \Delta\dot{\boldsymbol{\epsilon}} &= \frac{1}{2}\left(\Delta\eta\boldsymbol{I} - \boldsymbol{S}(\Delta\boldsymbol{\epsilon})\right)\Delta\boldsymbol{\omega} \\ \boldsymbol{J}\dot{\boldsymbol{\xi}} &= -\boldsymbol{S}(\boldsymbol{\xi})\boldsymbol{J}\boldsymbol{\omega} + \boldsymbol{Y}(\boldsymbol{\omega}, \boldsymbol{\omega}_{\mathrm{r}}, \dot{\boldsymbol{\omega}}_{\mathrm{r}})\boldsymbol{\theta} - \boldsymbol{\tau}.\end{aligned} \quad (17)$$

Since the inertial parameters of the quadrotor are unknown the following adaptive control is proposed

$$\boldsymbol{\tau} = \boldsymbol{Y}(\boldsymbol{\omega}, \boldsymbol{\omega}_{\mathrm{r}}, \dot{\boldsymbol{\omega}}_{\mathrm{r}})\widehat{\boldsymbol{\theta}} + \boldsymbol{K}_\xi\boldsymbol{\xi} + k_\epsilon\Delta\boldsymbol{\epsilon} \quad (18)$$

where $k_\epsilon \in \Re$ is a positive constant, $\boldsymbol{K}_\xi \in \Re^{3\times 3}$ is symmetric positive definite matrix and $\widehat{\boldsymbol{\theta}} \in \Re^p$ is an estimate of $\boldsymbol{\theta}$ which is updated according to

$$\dot{\widehat{\boldsymbol{\theta}}} = \boldsymbol{\Gamma}\boldsymbol{Y}^{\mathrm{T}}(\boldsymbol{\omega}, \boldsymbol{\omega}_{\mathrm{r}}, \dot{\boldsymbol{\omega}}_{\mathrm{r}})\boldsymbol{\xi} \quad (19)$$

where $\boldsymbol{\Gamma} \in \Re^{p\times p}$ is the adaptive gain.

4.3 Stability analysis

The main contribution of the paper is stated in the following theorem:

Theorem 1. For the quadrotor dynamics described by (1)-(3) with $\mathcal{Q}(0) = \{\eta(0), \boldsymbol{\epsilon}(0)\} \neq \{-1, \boldsymbol{0}\}$, the total thrust and the desired attitude given in (8) and (9) in combination with the linear observer (4), the auxiliary control (10) and the adaptive controller (18)-(19) guarante that all closed-loop variables are bounded and

$$\lim_{t\to\infty}\|\boldsymbol{x}\|_2 = 0, \quad \lim_{t\to\infty}\|\Delta\boldsymbol{\omega}\|_2 = 0, \quad \lim_{t\to\infty}\Delta\mathcal{Q} = \{1, \boldsymbol{0}\}$$

where $\boldsymbol{x} = \mathrm{col}(\Delta\boldsymbol{p}, \Delta\boldsymbol{v}, \widetilde{\boldsymbol{p}}, \widetilde{\boldsymbol{v}}) \in \Re^{12}$.

Proof. The first step of the proof consists in obtaining the closed-loop dynamics of the position and attitude errors. By taking into account (1), (7) and (10) the dynamics of the position and velocity errors are given by

$$\begin{aligned}\Delta\dot{\boldsymbol{p}} &= \widetilde{\boldsymbol{v}} \\ \Delta\dot{\boldsymbol{v}} &= -\boldsymbol{K}_1\Delta\boldsymbol{p} - \boldsymbol{K}_2\Delta\boldsymbol{v} - \boldsymbol{K}_1\widetilde{\boldsymbol{p}} \\ &\quad -\boldsymbol{K}_2\widetilde{\boldsymbol{v}} - \frac{\mathcal{T}}{m}(\boldsymbol{R} - \boldsymbol{R}_{\mathrm{d}})\boldsymbol{z}_0.\end{aligned} \quad (20)$$

The interconnection term $(\boldsymbol{R} - \boldsymbol{R}_{\mathrm{d}})\boldsymbol{z}_0$ can be written as

$$(\boldsymbol{R} - \boldsymbol{R}_{\mathrm{d}})\boldsymbol{z}_0 = \boldsymbol{R}(\boldsymbol{I} - \Delta\boldsymbol{R}(\Delta\eta, \Delta\boldsymbol{\epsilon}))\boldsymbol{z}_0 = \boldsymbol{R}\boldsymbol{S}(\bar{\boldsymbol{\epsilon}})\Delta\boldsymbol{\epsilon} \quad (21)$$

where $\bar{\boldsymbol{\epsilon}} \triangleq \mathrm{col}(\Delta\epsilon_{\mathrm{y}}, -\Delta\epsilon_{\mathrm{x}}, \Delta\eta)$. Equations (5) and (20) admit the following state-space representation

$$\dot{\boldsymbol{x}} = \boldsymbol{A}\boldsymbol{x} + \boldsymbol{B}\frac{\mathcal{T}}{m}\boldsymbol{R}\boldsymbol{S}(\bar{\boldsymbol{\epsilon}})\Delta\boldsymbol{\epsilon} \quad (22)$$

where

$$\boldsymbol{A} = \left[\begin{array}{cc|cc} \boldsymbol{O}_{3\times3} & \boldsymbol{I} & \multicolumn{2}{c}{\boldsymbol{O}_{3\times6}} \\ -\boldsymbol{K}_1 & -\boldsymbol{K}_2 & -\boldsymbol{K}_1 & -\boldsymbol{K}_2 \\ \hline \multicolumn{2}{c|}{\multirow{2}{*}{\boldsymbol{O}_{6\times6}}} & -\boldsymbol{L}_1 & \boldsymbol{I} \\ & & -\boldsymbol{L}_2 & \boldsymbol{O}_{3\times3} \end{array}\right], \quad \boldsymbol{B} = \begin{bmatrix} \boldsymbol{O}_{3\times3} \\ \boldsymbol{I} \\ \boldsymbol{O}_{6\times3} \end{bmatrix} \tag{23}$$

where $\boldsymbol{O}_{n\times n}$ denotes a zero matrix of dimension $n \times n$.

On the other hand, by substituting the adaptive controller (18)-(19) into (17) we obtain the closed-loop dynamics for the attitude subsystem given by

$$\begin{aligned} \Delta\dot{\eta} &= -\frac{1}{2}\Delta\boldsymbol{\epsilon}^{\mathrm{T}}\Delta\boldsymbol{\omega} \\ \Delta\dot{\boldsymbol{\epsilon}} &= \frac{1}{2}\left(\Delta\eta\boldsymbol{I} - \boldsymbol{S}(\Delta\boldsymbol{\epsilon})\right)\Delta\boldsymbol{\omega} \\ \boldsymbol{J}\dot{\boldsymbol{\xi}} &= -\boldsymbol{S}(\boldsymbol{\xi})\boldsymbol{J}\boldsymbol{\omega} + \boldsymbol{Y}_{\mathrm{r}}\Delta\boldsymbol{\theta} - \boldsymbol{K}_\xi\boldsymbol{\xi} - k_\epsilon\Delta\boldsymbol{\epsilon} \\ \Delta\dot{\boldsymbol{\theta}} &= -\boldsymbol{\Gamma}\boldsymbol{Y}_{\mathrm{r}}^{\mathrm{T}}\boldsymbol{\xi} \end{aligned} \tag{24}$$

where $\boldsymbol{Y}_{\mathrm{r}} = \boldsymbol{Y}(\boldsymbol{\omega}, \boldsymbol{\omega}_{\mathrm{r}}, \dot{\boldsymbol{\omega}}_{\mathrm{r}})$ and $\Delta\boldsymbol{\theta} = \boldsymbol{\theta} - \widehat{\boldsymbol{\theta}}$ is the parametric error. Equations (20) and (22) describe the closed-loop error dynamics of the whole system.

Since (24) does not depend on the state $\boldsymbol{x}$, the second step of the proof consists in analyzing the stability of the equilibrium point $(\Delta\eta, \Delta\boldsymbol{\epsilon}, \boldsymbol{\xi}, \Delta\boldsymbol{\theta}) = (1, \boldsymbol{0}, \boldsymbol{0}, \boldsymbol{0})$. To this end, consider the positive scalar function

$$V_{\mathrm{a}} = \frac{1}{2}\boldsymbol{\xi}^{\mathrm{T}}\boldsymbol{J}\boldsymbol{\xi} + \frac{1}{2}\Delta\boldsymbol{\theta}^{\mathrm{T}}\boldsymbol{\Gamma}^{-1}\Delta\boldsymbol{\theta} + 2k_\epsilon(1 - \Delta\eta) \tag{25}$$

whose time derivative along (24) is given by

$$\dot{V}_{\mathrm{a}} = -\boldsymbol{\xi}^{\mathrm{T}}\boldsymbol{K}_\xi\boldsymbol{\xi} - k_\epsilon\Delta\boldsymbol{\epsilon}^{\mathrm{T}}\boldsymbol{\xi} + k_\epsilon\Delta\boldsymbol{\epsilon}^{\mathrm{T}}\Delta\boldsymbol{\omega} \tag{26}$$

By taking into account (16) $\dot{V}_{\mathrm{a}}$ becomes

$$\dot{V}_{\mathrm{a}} = -\boldsymbol{\xi}^{\mathrm{T}}\boldsymbol{K}_\xi\boldsymbol{\xi} - k_\epsilon^2\|\Delta\boldsymbol{\epsilon}\|_2^2 \leq -\underline{k}\|\boldsymbol{r}\|_2^2 \leq 0 \tag{27}$$

where $\boldsymbol{r} = \mathrm{col}(\|\boldsymbol{\xi}\|_2, \|\Delta\boldsymbol{\epsilon}\|_2)$ and $\underline{k} = \min\{\lambda_{\min}\{\boldsymbol{K}_\xi\}, k_\epsilon^2\}$. Therefore, the closed-loop variables $\Delta\eta$, $\Delta\boldsymbol{\epsilon}$, $\boldsymbol{\xi}$ and $\Delta\boldsymbol{\theta}$ are bounded. This in turn implies that $\Delta\boldsymbol{\omega}$ is also bounded (see (16)). Integrating both sides of (27) yields

$$V_{\mathrm{a}}(t) - V_{\mathrm{a}}(0) \leq -\underline{k}\int_0^t \|\boldsymbol{r}(\vartheta)\|_2 \mathrm{d}\vartheta \tag{28}$$

Since V_{a} is nonincreasing, one has

$$\int_0^t \|\boldsymbol{r}(\vartheta)\|_2 \mathrm{d}\vartheta \leq \frac{1}{\underline{k}}V_{\mathrm{a}}(0). \tag{29}$$

The previous result shows that $\boldsymbol{r} \in \mathcal{L}_2 \cap \mathcal{L}_\infty$, this implies that $\boldsymbol{\xi}$, $\Delta\boldsymbol{\epsilon}$, and $\Delta\boldsymbol{\omega}$ converge asymptotically to zero. Since the quaternion error satisfies $\Delta\eta^2 + \|\Delta\boldsymbol{\epsilon}\|_2^2 = 1$ and assuming that $\Delta\eta(0) \neq -1$ it is concluded that $\Delta\eta \to 1$ as $t \to \infty$.

The final step of the proof consists in showing that $\lim_{t\to\infty}\|\boldsymbol{x}\|_2 = 0$. It is worth to mention that the control and observer gains $\boldsymbol{K}_i$ and $\boldsymbol{L}_i$ $(i = 1, 2)$ can be chosen such that the matrix $\boldsymbol{A}$ in (22) is Hurtwitz. Consider the candidate Lyapunov function $V_{\mathrm{p}} = \boldsymbol{x}^{\mathrm{T}}\boldsymbol{P}\boldsymbol{x}$ where $\boldsymbol{P} \in \Re^{12\times12}$ is a symmetric positive matrix which satisfies $\boldsymbol{P}\boldsymbol{A} + \boldsymbol{A}^{\mathrm{T}}\boldsymbol{P} = -q\boldsymbol{I}$, for $q > 0$. The time derivative of V_{p} along (22) is given by

$$\dot{V}_{\mathrm{p}} = -q\|\boldsymbol{x}\|_2^2 + \frac{2}{m}\mathcal{T}\boldsymbol{x}^{\mathrm{T}}\boldsymbol{P}\boldsymbol{B}\boldsymbol{R}\boldsymbol{S}(\bar{\boldsymbol{\epsilon}})\Delta\boldsymbol{\epsilon}. \tag{30}$$

By taking into account (8) and (10) an upper bound of $\mathcal{T}$ can be computed as

$$\mathcal{T} = m\|\boldsymbol{u} + g\boldsymbol{z}_0\| \leq m(\|\dot{\boldsymbol{v}}_{\mathrm{d}}\|_\infty + g) + 2m\bar{k}\|\boldsymbol{x}\|_2 \tag{31}$$

Table 1. Control/observer parameters

Position/Observer		Orientation/Adaptive	
Gain	Value	Gain	Value
$\boldsymbol{K}_1$	diag(4, 3, 15)	$\boldsymbol{K}_\xi$	diag(3, 3, 3)
$\boldsymbol{K}_2$	diag(5, 3.5, 8)	k_ϵ	2
$\boldsymbol{L}_1$	diag(10, 15, 16)	$\boldsymbol{\Gamma}$	diag(0.02, 0.02, 0.01)
$\boldsymbol{L}_2$	diag(16, 36, 60)	λ	5

where $\bar{k} = \max\{\lambda_{\max}\{\boldsymbol{K}_1\}, \lambda_{\max}\{\boldsymbol{K}_2\}\}$. Based on the previous analysis it can be shown that

$$\mathcal{T} \leq \begin{cases} mc\|\boldsymbol{x}\|_2, & \text{if } \|\boldsymbol{x}\|_2 \geq a \\ mca, & \text{if } \|\boldsymbol{x}\|_2 < a \end{cases} \tag{32}$$

with $a \triangleq (\|\dot{\boldsymbol{v}}\|_\infty + g)/2\bar{k}$ and $c \triangleq 4\bar{k}$. Since $\|\boldsymbol{B}\|_2 = 1$, $\|\boldsymbol{R}\|_2 = 1$, $\|\boldsymbol{S}(\bar{\boldsymbol{\epsilon}})\|_2 = \|\bar{\boldsymbol{\epsilon}}\|_2 \leq 1$ and by taking into account (32) the time derivative of V_{p} satisfies

$$\dot{V}_{\mathrm{p}} \leq -\left(q - 2\lambda_{\max}\{\boldsymbol{P}\}c\|\Delta\boldsymbol{\epsilon}\|_2\right)\|\boldsymbol{x}\|_2, \quad \forall\|\boldsymbol{x}\|_2 \geq a \tag{33}$$

Since $\|\Delta\boldsymbol{\epsilon}\|_2 \to 0$ as $t \to \infty$ there exist a finite period such that

$$\|\Delta\boldsymbol{\epsilon}\|_2 = \frac{q}{4\lambda_{\max}\{\boldsymbol{P}\}c} \implies \dot{V}_{\mathrm{p}} \leq -\frac{1}{2}q\|\boldsymbol{x}\|_2^2. \tag{34}$$

Therefore, $\boldsymbol{x}(t)$ is bounded and converges asymptotically (exponentially) to zero. This completes the proof. □

5. SIMULATION RESULTS

The performance of the proposed control algorithm is evaluated by means of numerical simulations. The parameters of the quadrotor used in the simulation are $m = 1$[Kg], $g = 9.8$[m/s^2] and $\boldsymbol{J} = \mathrm{diag}(\theta_1, \theta_2, \theta_3) = (0.01, 0.05, 0.05)$[Kgm^2]. The initial position and orientation of the aerial robot are $\boldsymbol{p}(0) = \mathrm{col}(2.5, 2.5, 0)$[m], $\eta(0) = 0.8924$, $\boldsymbol{\epsilon} = \mathrm{col}(0, 0.2588, 0.3696)$, respectively. It is assumed that the vehicle starts its motion from rest, *i.e.*, $\boldsymbol{v}(0) = \boldsymbol{0}$ and $\boldsymbol{\omega}(0) = \boldsymbol{0}$. The initial guess of the inertial parameters is $\widehat{\boldsymbol{\theta}} = \boldsymbol{0}$. Finally, the control, observer, and adaptation gains are shown in Table 1.

The structure of the regressor matrix in (18) is the following

$$\boldsymbol{Y}(\boldsymbol{\omega}, \boldsymbol{\omega}_{\mathrm{r}}, \dot{\boldsymbol{\omega}}_{\mathrm{r}}) = \begin{bmatrix} \dot{\omega}_{\mathrm{rx}} & -\omega_{\mathrm{y}}\omega_{\mathrm{rz}} & \omega_{\mathrm{z}}\omega_{\mathrm{ry}} \\ \omega_{\mathrm{x}}\omega_{\mathrm{rz}} & \dot{\omega}_{\mathrm{ry}} & -\omega_{\mathrm{z}}\omega_{\mathrm{rx}} \\ -\omega_{\mathrm{x}}\omega_{\mathrm{ry}} & \omega_{\mathrm{y}}\omega_{\mathrm{rx}} & \dot{\omega}_{\mathrm{rz}} \end{bmatrix} \tag{35}$$

with $\boldsymbol{\omega} = \mathrm{col}(\omega_{\mathrm{x}}, \omega_{\mathrm{y}}, \omega_{\mathrm{z}})$ and $\boldsymbol{\omega}_{\mathrm{r}} = \mathrm{col}(\omega_{\mathrm{rx}}, \omega_{\mathrm{ry}}, \omega_{\mathrm{rz}})$.

The desired position is given by

$$\boldsymbol{p}_{\mathrm{d}} = \begin{bmatrix} 3\cos(2\pi t/40) \\ 3\sin(2\pi t/40) \\ 0.5\cos(2\pi t/10) + 2 \end{bmatrix} [\mathrm{m}]. \tag{36}$$

The quadrotor's trajectory is shown in Fig. 2. After the transient response a good tracking is achieved. The Fig. 3 shows the euclidean norms of the position and observation errors. As it can be appreciated, both errors converge asymptotically to zero. The trajectory tracking performance in the orientation subspace is depicted in Fig. 4. From the figure, it is clear that the norm of the vector part of the unit quaternion converges to zero and the scalar part converges to one, thus, a good attitude tracking is also achieved.

Finally, the estimated inertial parameters and the control inputs are shown in Figures 5 and 6, respectively. Notice

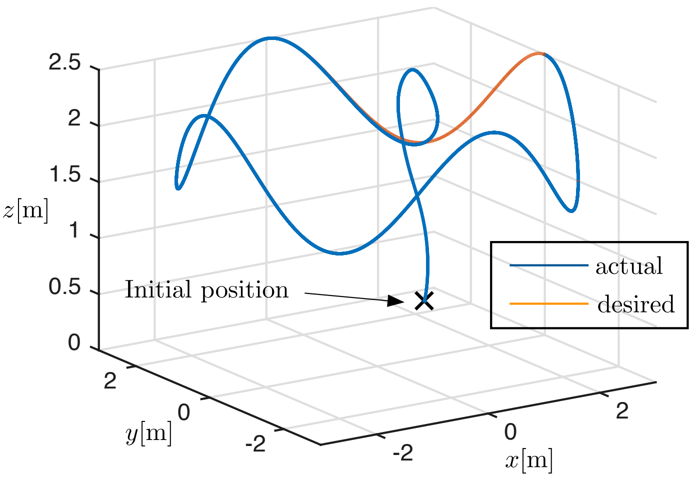

Fig. 2. Quadrotor's trajectory in 3D

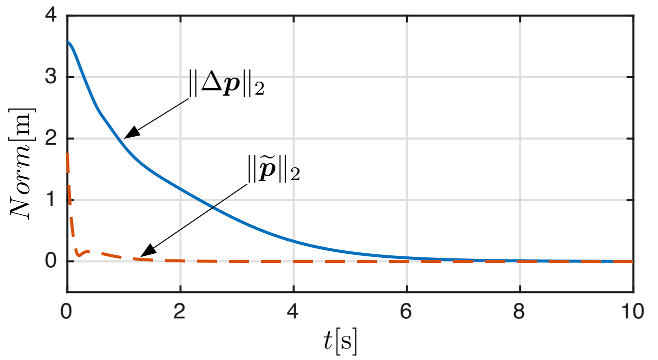

Fig. 3. Norm of the position $\Delta \boldsymbol{p}$ and observation $\widetilde{\boldsymbol{p}}$ errors

that the estimated parameters do not converge to the real ones, this due to the desired trajectory is not a persistently exciting function. However, this is not drawback, since the main objective is trajectory tracking rather than exact parameter estimation. Since the initial position and observer error are relatively large, the proposed control-observer algorithm requires more control effort at the beginning of the trajectory. After the transient response, the total thrust is about 10[N] and the norm of the input torque is about ± 0.02[N·m].

6. CONCLUSIONS

In this paper, the problem of position trajectory tracking of a quadrotor in a 3D environment with model parameter uncertainties and without using linear velocity measurements was addressed. Due to the cascade nature of the quadrotor's dynamics, a hierarchical control strategy was proposed. To avoid the singularities of the Euler angles, the attitude adaptive controller was designed based on the unit quaternion. On the other hand, a simple Luenberger observer was presented to estimate the linear velocity of the aircraft. The stability analysis of the closed-loop system was carried out by means of Lyapunov theory and the stability properties of cascade systems. Simulations results show the performance of the proposed control algorithm. Some future work include: experimental validation of the proposed control-observer algorithm, inclusion of the actuator dynamics in the control design, and designing

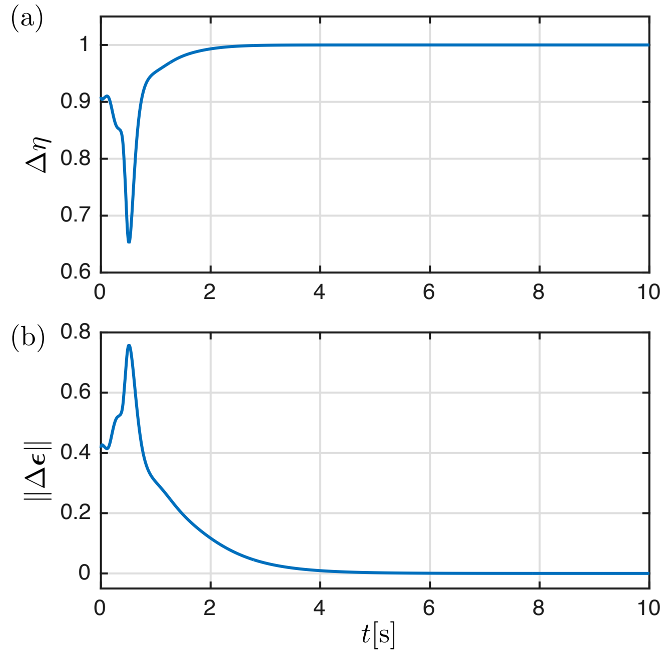

Fig. 4. Time evolution of the unit quaternion error: (a) $\Delta\eta$, (b) $\|\Delta\boldsymbol{\epsilon}\|$

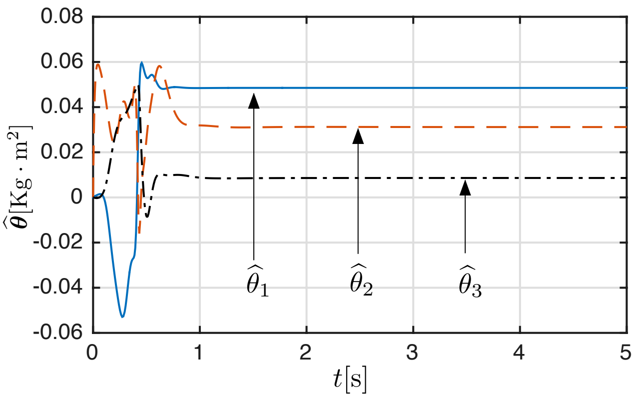

Fig. 5. Time evolution of the estimated parameters

robust control algorithms capable of handling external disturbances.

REFERENCES

Abdessameud, A. and Tayebi, A. (2009). Formation control of VTOL UAVs. In *Proceedings of the 48th IEEE Conference On Decison and Control*, 3454–3459.

Abdessameud, A. and Tayebi, A. (2010). Global trajectory tracking control of vtol-uavs without linear velocity a. global trajectory tracking control of vtol-uavs without linear velocity. *Automatica*, 46(6), 1053–1059.

Bouabdallah, S., North, A., and Siegwart, R. (2004). PID vs LQ control techniques applied to an indoor micro quadrotor. In *Proceedings of the IEEE/RSJ International Conference on Intelligent Robots and Systems*, volume 3, 2451–2456.

Castillo, P., Lozano, R., and Dzul, A. (2005). Stabilization of a mini rotorcraft with four rotors. *IEEE Control Systems Magazine*, 25(6), 45–55.

Dydek, Z., Annaswamy, M., and Lavrestky, E. (2013). Adaptive control of quadrotor uavs: A design trade

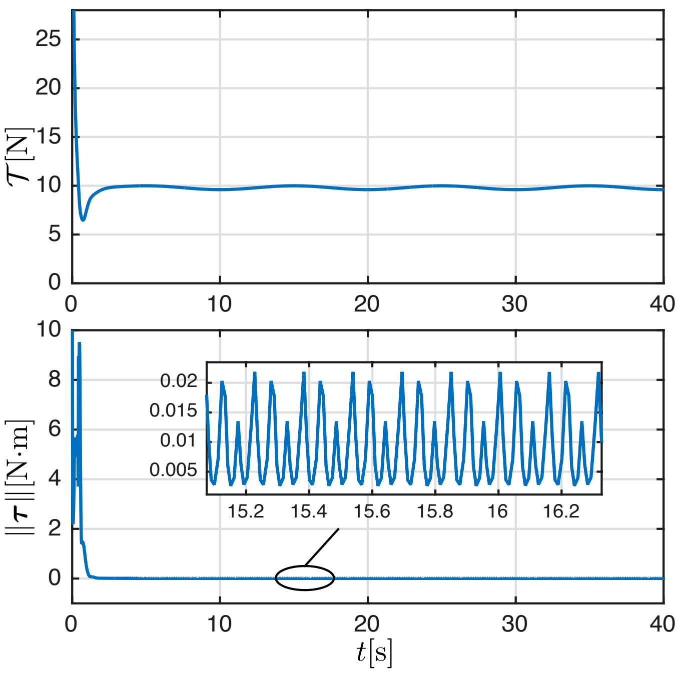

Fig. 6. Control inputs: (a) total thrust $\mathcal{T}$, (b) norm of the input torque $\boldsymbol{\tau}$

study with flight evaluations. *IEEE Transactions on Control Systems Technology*, 21(4), 1400–1406.

Ha, C., Zuo, Z., Choi, F., and Lee, D. (2014). Passivity-based adaptive backstepping control of quadrotor-type UAVs. *Robotics and Autonomous Systems*, 62(9), 1305–1315.

How, J., Bethke, B., Frank, A., Dale, D., and Vian, J. (2008). Real-time indoor autonomous vehicle test environment. *IEEE Control Systems Magazine*, 28(2), 51–64.

Kendoul, F., Yu, Z., and Nonami, K. (2010). Guidance and nonlinear control system for autonomous flight of minirotorcraft unmanned aerial vehicles. *Journal of Field Robotics*, 27(3), 311–334.

Lee, D., Kim, H., and Sastry, S. (2009). Feedback linearization vs. adaptive sliding mode control for a quadrotor helicopter. *International Journal of Control Automation and Systems*, 7(3), 419–428.

Lee, T., Leok, M., and McClamroch, N. (2010). Geometric tracking control of a quadrotor uav on se(3). In *Proceedings of the 49th IEEE Conference on Decision and Control*, 5420–5425.

Mahoney, R., Kumar, V., and Corke, P. (2012). Multirotor aerial vehicles modeling, estimation, and control of quadrotor. *IEEE Robotics and Automation Magazine*, 19(3), 20–32.

Mellinger, D., Michael, N., and Kumar, V. (2012). Trajectory generation and control for precise aggressive maneuvers with quadrotors. *International Journal of Robotics Research*, 31(5), 664–674.

Michael, N., Mellinger, D., Lindsey, Q., and Kumar, V. (2010). The GRASP multiple micro-UAV test bed experimental evaluation of multirobot aerial control algorithms. *IEEE Robotics and Automation Magazine*, 17(3), 56–65.

Pounds, P., Mahoney, R., and Corke, P. (2006). Modelling and control of a quad-rotor robot. In *Proceedings of the Australasian Conference on Robotics and Automation*.

Rosaldo-Serrano, M., Santiaguillo-Salinas, J., and Aranda-Bricaire, E. (2019). Observer-based time-varying backstepping control for a quadrotor multi-agent system. *Journal of Intelligent and Robotic Systems*, 93(1-2), 135–150.

Siciliano, B. and Villani, L. (1999). *Robot force control.* Springer.

Tayebi, A. and McGilvray, S. (2006). Attitude stabilization of a VTOL quadrotor aircraft. *IEEE Transactions on Control Systems Technology*, 14(3), 562–571.

Zou, Y. (2017a). Nonlinear robust adaptive hierarchical sliding mode control approach for quadrotors. *International Journal of Robust and Nonlinear Control*, 27(6), 925–941.

Zou, Y. (2017b). Trajectory tracking controller for quadrotors without velocity and angular velocity measurements. *IET Control Theory and Applications*, 11(1), 101–109.

Zuo, Z. (2010). Trajectory tracking control design with command-filtered compensation for a quadrotor. *IET Control Theory and Applications*, 4(11), 2343–2355.